QUANTIFYING LOW ENERGY PROTON DAMAGE IN MULTIJUNCTION SOLAR CELLS

Scott R. Messenger
SFA Inc., Crofton, MD 21114

Edward A. Burke
Consultant, Woburn, MA 01801

Robert J. Walters
US Naval Research Laboratory, Washington, DC 20375

Jeffrey H. Warner
US Naval Research Laboratory, Washington, DC 20375

Geoffrey P. Summers
US Naval Research Laboratory, Washington, DC 20375
University of Maryland Baltimore County, Baltimore, MD 21250

Justin R. Lorentzen
SFA Inc., Crofton, MD 21114

Thomas L. Morton
Ohio Aerospace Institute, Cleveland, OH 44142

Steven J. Taylor
European Space Agency, ESTEC, Noordwijk, The Netherlands

ABSTRACT

An analysis of the effects of low energy proton irradiation on the electrical performance of triple junction (3J) $InGaP_2$/GaAs/Ge solar cells is presented. The Monte Carlo ion transport code (SRIM) is used to simulate the damage profile induced in a 3J solar cell under the conditions of typical ground testing and that of the space environment. The results are used to present a quantitative analysis of the defect, and hence damage, distribution induced in the cell active region by the different radiation conditions. The modelling results show that, in the space environment, the solar cell will experience a uniform damage distribution through the active region of the cell. Through an application of the displacement damage dose analysis methodology, the implications of this result on mission performance predictions are investigated.

1. INTRODUCTION

A multijunction (MJ) solar cell consists of two or more p-n junctions stacked on top of one another, where the thickness and bandgap of each subcell is specifically chosen to maximize absorption of the illumination source spectrum. In this discussion, we focus on the $InGaP_2$/GaAs/Ge triple-junction (3J) technology. In space, the illumination spectrum is the air mass zero (AM0) spectrum (Figure 1). A measurement of the quantum efficiency (QE) (a measure of how efficiently a solar cell converts individual wavelengths of light into electricity) of a 3J $InGaP_2$/GaAs/Ge cell shows how the spectral response of this technology overlaps the AM0 spectrum, thereby enabling better light collection than single junction devices.

An MJ cell is a series-connected device. The total device photovoltage is the sum of photovoltages from each subcell. The MJ device photocurrent, however, is limited to the least value of the three subcells, which is referred to as the "current limiter". As a result, the radiation response of the MJ device is primarily controlled by the most radiation sensitive subcell, which is the GaAs subcell (Figure 1) for the 3J $InGaP_2$/GaAs/Ge. The structure of the 3J cell can be engineered to control the radiation resistance to some extent. The most common method used for this has been to thin the top $InGaP_2$ cell, thereby forcing the 3J cell to be current limited at beginning of life (BOL) by the more radiation hard $InGaP_2$ top cell. However, the trade-off is a slightly reduced BOL conversion efficiency.

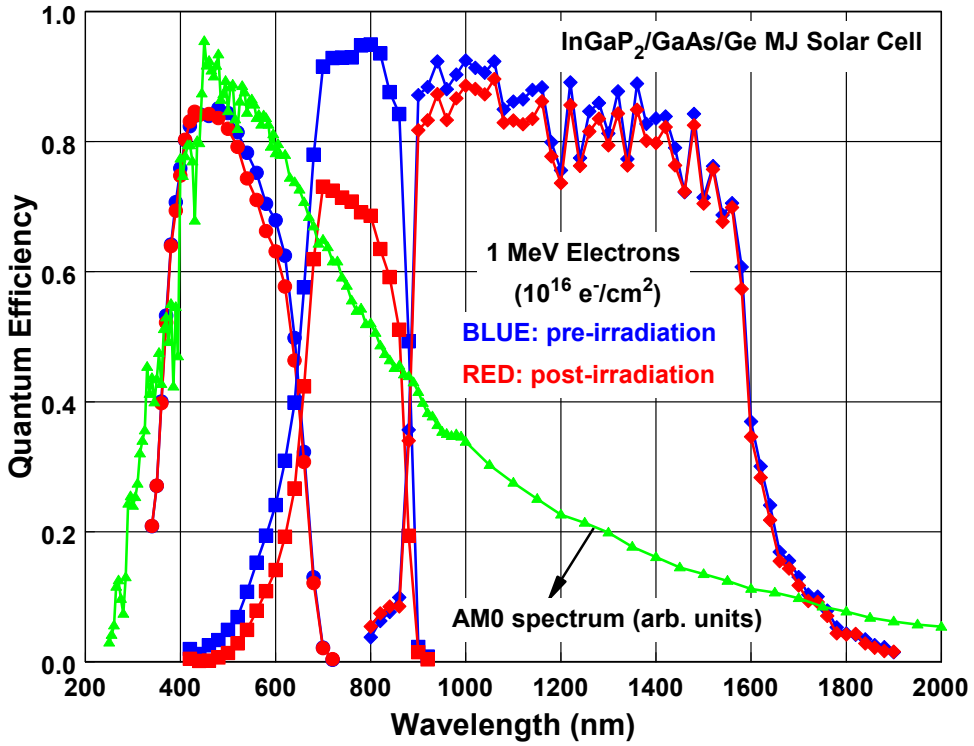

Figure 1: AM0 solar spectrum, normalized to the maximum irradiance value with QE data from a 3J $InGaP_2$/GaAs/Ge solar cell measured before and after electron irradiation. The middle GaAs cell is the most radiation sensitive subcell.

While this technique has been proven to render the 3J device more resistant to 1 MeV electron radiation, the specific case of low energy proton irradiation has remained a point of discussion. Protons with incident energies of about 200 keV or less have the potential to decelerate (slow-down) and stop within one of subcells, and may preferentially degrade one junction over the others. This may have a significant impact on the balancing of the photocurrents and, therefore, the overall device radiation response.

This paper presents a modelling study designed to quantify low energy proton irradiation effects in 3J $InGaP_2$/GaAs/Ge solar cells. Using the Monte Carlo ion transport code SRIM[1], we quantify low energy proton effects by calculating the amount of displacement damage absorbed within each layer of the 3J device due to various energy proton irradiations and calculating the expected solar cell degradation using the displacement damage dose (D_d) analysis methodology [2,3].

This modelling is performed for several cases. The first one is the case of a monoenergetic, unidirectional beam of protons normally incident upon an uncovered solar cell, representative of a typical radiation ground test. This modelling is repeated for the same monoenergetic proton beam except that the protons are assumed to be omnidirectional. As a third case, an omnidirectional spectrum of protons that has been modified to reflect transport through a coverglass is modelled. This case is representative of the true space radiation environment. These cases were specifically chosen to bridge the gap between ground test results and the degradation expected to be seen on-orbit.

The analysis highlights the different defect structure induced by an omnidirectional as compared to a unidirectional irradiation. Furthermore, the defect structure induced within a covered solar cell after exposure to an omnidirectional

spectrum of protons is compared to the unidirectional, monoenergetic case. The data are used to demonstrate that the localized defect structure induced at the end of a proton track clearly observed after monoenergetic, unidirectional irradiation of an uncovered solar cell is not evident within a covered solar cell exposed to an omnidirectional spectrum of protons. The implications of this result on ground test and on-orbit predictions are discussed.

2. DISPLACEMENT DAMAGE EFFECTS

As a charged particle passes through a material, it transfers energy to the crystal lattice through either ionization or atomic displacements. Whereas ionization damage dominates the particle range in a material, it is the displacement damage that causes the degradation of the photovoltaic output of a solar cell, as the introduction of point defects (vacancies, interstitials, etc.) gives rise to recombination centers that degrade the minority carrier diffusion length [4,5,6].

The rate at which an irradiating particle transfers displacement damage energy to the target lattice is referred to as the nonionizing energy loss (NIEL), which can be calculated analytically based on the displacement interaction cross sections [7,8]. The NIEL for protons and electrons incident upon the three materials of a 3J $InGaP_2$/GaAs/Ge solar cell are shown in Figure 2. The NIEL values are quite similar for the three materials since the interaction cross sections vary with the average atomic number of the material which are essentially equal amongst the three.

The proton NIEL increases with decreasing energy. Thus, lower energy protons produce more displacement damage. Furthermore, as the proton slows down, its energy decreases further and the NIEL increases accordingly. This process continues until the proton eventually comes to rest. As a result, lower energy protons create more damage culminating in a peak in the defect concentration at the end of the proton track. This peak is referred to as the Bragg peak. For a specific range of incident proton energies, the Bragg peak may occur within the active region of the solar cell. Moreover, the Bragg peak may occur within one of the subjunctions of the 3J device. It is the response of the 3J device to such a radiation exposure that is the focus of the analysis of this paper.

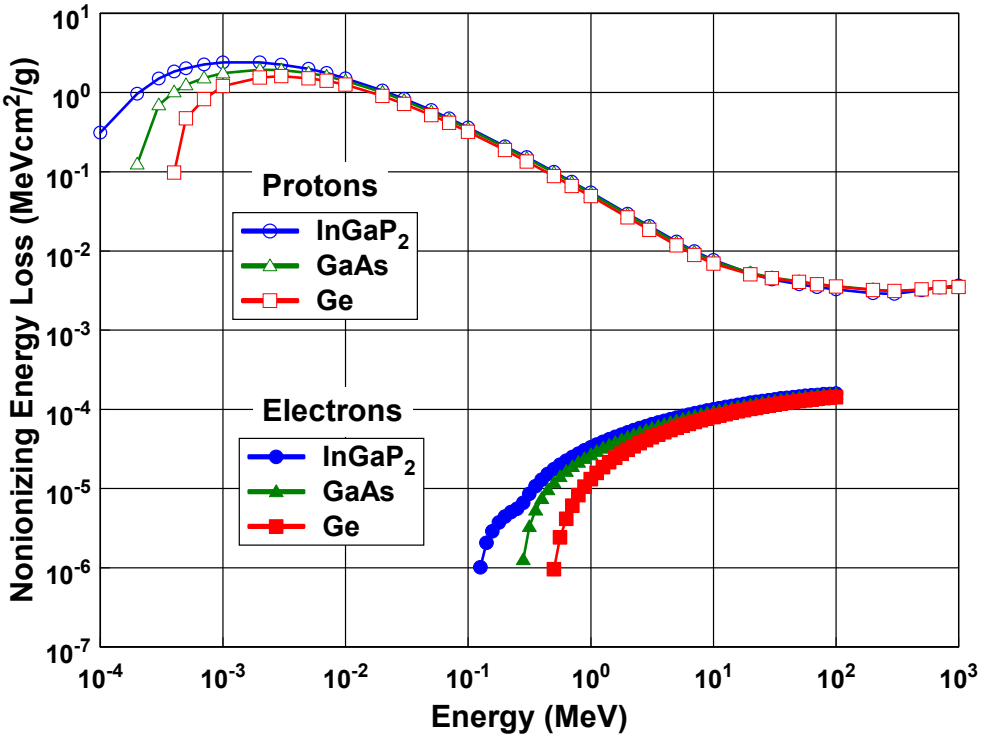

Figure 2: NIEL calculated for electrons and protons incident upon $InGaP_2$, GaAs, and Ge.

3. SPACE RADIATION ENVIRONMENT

The space radiation environment is a dynamic mixture of protons and electrons that varies with orbital altitude and inclination. To model on-orbit solar cell performance, a specific orbit must be chosen. Here, we choose an orbit containing the L2 point. This is one of the so-called Lagrangian points [9]. This orbit places the spacecraft outside of the Earth's magnetic field. Therefore, the solar arrays will have no geomagnetic shielding, and the solar cell damage will be dominated by exposure to protons from solar events. In the case of the geosynchronous orbit, the proton contribution is essentially the same, but trapped electrons are also important. The conclusions drawn here apply to other missions for which trapped protons are important, since the trapped proton spectrum is generally similar to the solar proton spectrum.

The differential proton spectrum as obtained using SPENVIS [10] after 3.5 years in this orbit is shown in Figure 3. These data represent the omnidirectional, isotropic radiation environment in which the solar array will be immersed. Before penetrating the solar cell active region, the proton spectrum must pass through the coverglass and any surface layers on the front, and the array structure and cell substrate on the back. Following the theory of the previous section, the protons will lose energy and decelerate through the shielding materials, thus the spectrum incident upon the cell active region will be slowed-down. The slowed down spectrum emerging from the shielding material can be calculated both by analytical and Monte Carlo means.

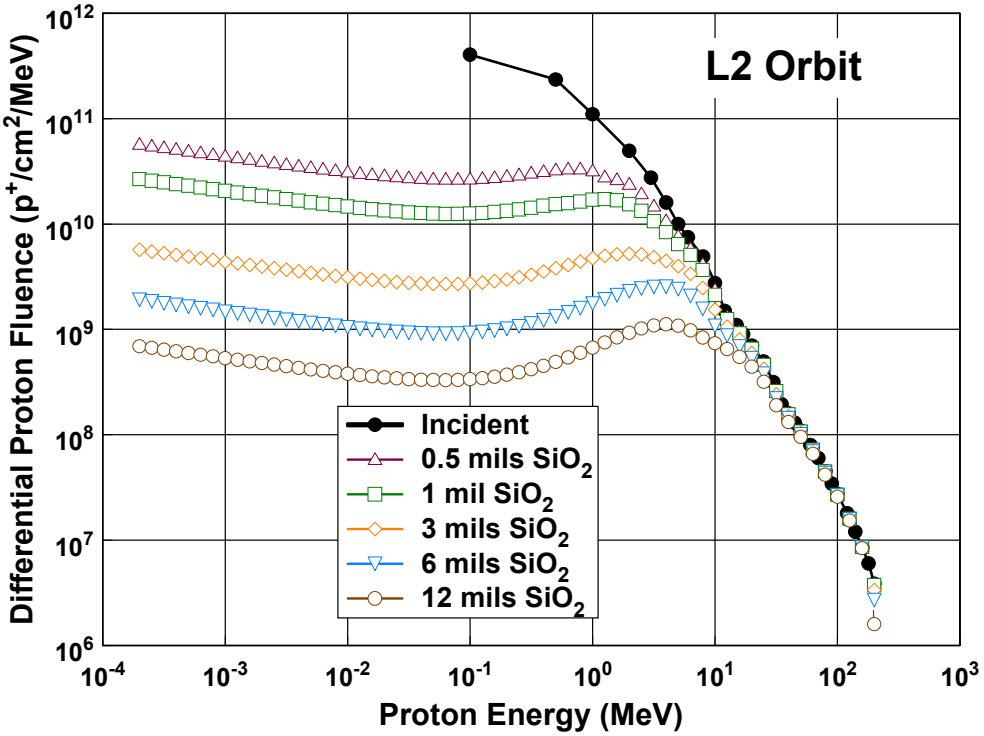

Figure 3: Proton spectra calculated after 3.5 years in the L2 obit for various thicknesses of SiO_2 coverglass.

The slowed-down spectra shown in Figure 3 were calculated by applying the continuous slowing down approximation [11,12,13], and these results have been confirmed by calculations using the software code MULASSIS [14,9]. Considering only front-side exposure, the calculations are performed over all incident angles, and results are shown for several SiO_2 coverglass thickness. To include the back-side exposure component, the array substrate material is typically expressed as an equivalent thickness of coverglass and the calculations are repeated. The results are then added to the front-side spectrum to give the total slowed-down spectrum.

Assuming that the total equivalent shielding thickness is equal to a coverglass thickness given in Figure 3, the corresponding slowed-down spectrum represents the protons incident directly upon the cell active region. The slowed-down spectrum is omnidirectional. For an L2 or a GEO mission, a coverglass is typically 75-150 μm (3-6 mils) thick,

and an Al honeycomb solar array substrate is equivalent to a coverglass thickness on the order of 750 μm (30 mils) [1]. Since the 3J cell active region is typically < 10 μm, the slowed-down spectrum will not change appreciably as it passes through the active layers and can be considered constant as was verified in the calculations in [5].

4. MODELLING RESULTS

4.1 Monoenergetic, Unidirectional Protons

For the present calculations, we choose a solar cell structure where the $InGaP_2$, GaAs, and Ge layers are 0.5, 3, and 500 μm, respectively. To calculate the damage induced within the solar cell due to proton irradiation, we have used the SRIM Monte Carlo program [1]. The first case modelled was that of a monoenergetic, unidirectional beam of protons normally incident upon the surface of the solar cell. Some SRIM results (vacancy.txt) are shown in Figure 4.

The data in Figure 4 give the rate at which vacancies are produced per incident proton along the proton track through the material. Integrating with respect to depth into the sample gives the total vacancy concentration, or equivalently the total displacement damage induced in the cell per incident ion, which can be directly related to solar cell degradation as described in [15,16].

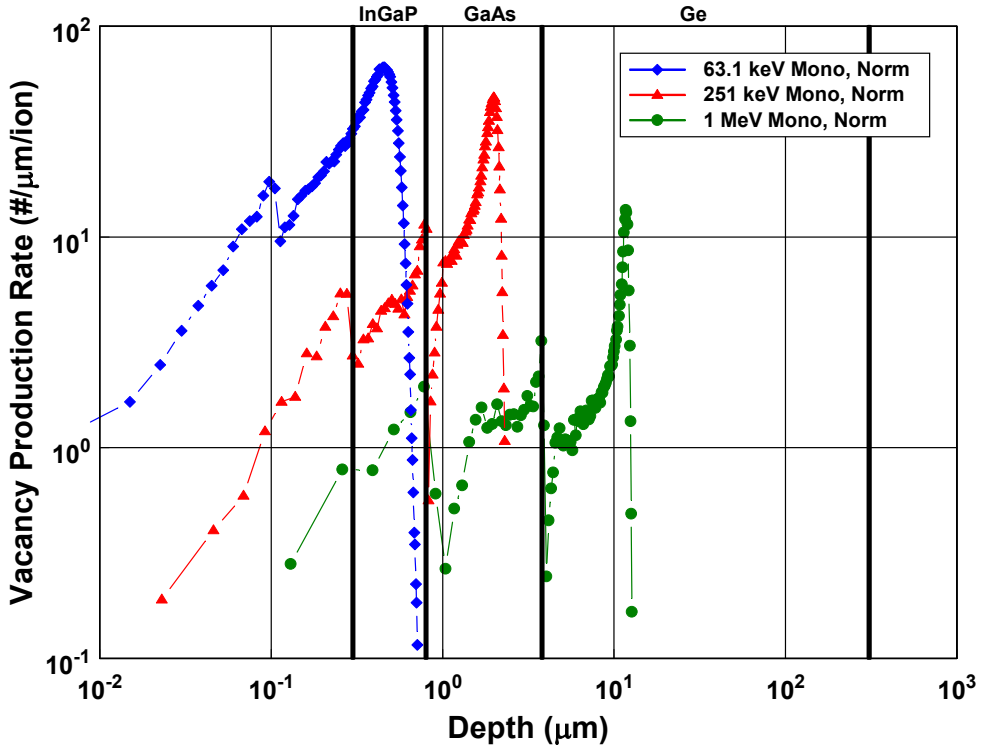

Figure 4: Vacancy production rate throughout a 3J solar cell by normally incident, monoenergetic, unidirectional proton irradiation as calculated by SRIM [1].

The data of Figure 4 illustrate the slowing down of the protons as they traverse the solar cell material, with the Bragg peak appearing at the end of the proton track. The different irradiations produce different defect distributions, and these distributions are non-uniform throughout the cell active region. As a result, the solar cell response to each individual irradiation will be different. Irradiation by protons with the lowest incident energy that stop nearest the surface (63 keV) will affect only the $InGaP_2$ subcell. Irradiation by protons with incident energy of 251 keV protons, however, will affect both the $InGaP_2$ and GaAs subcells but not the Ge. Also, with the Bragg peak occurring in the GaAs layer, the 251 keV irradiations may preferentially degrade the GaAs. Irradiation by protons with incident energy of 1 MeV and above, on the other hand, produces nearly uniform damage throughout the entire active region.

These effects have been shown explicitly in [2] and by the data produced by Sumita et al. [17] as shown in Figure 5. Figure 5 shows the maximum power output (P_{max}) measured in 3J $InGaP_2$/GaAs/Ge solar cells after unidirectional, normally incident irradiations by monoenergetic protons. The incident energy of each proton irradiation is given in the legend. These solar cells were uncovered during the irradiations. Following the methodology of Messenger et al. [3], the data are plotted as a function of D_d which is given by the product of the particle fluence and the NIEL (Figure 2). Analyses in terms of D_d allow data measured after irradiation by different particles at different energies to be correlated and presented on a common axis [2,18].

Their data show two general groupings. For unidirectional, normally incident protons with incident energies of 0.1 MeV and below, the protons stop within the top subcell and the 3J cell response tracks that of the more radiation resistant $InGaP_2$ subcell (solid symbols in Figure 5). For higher incident energies, the protons penetrate the middle subcell, and the 3J cell response tracks that of the less resistant GaAs subcell (open symbols in Figure 5).

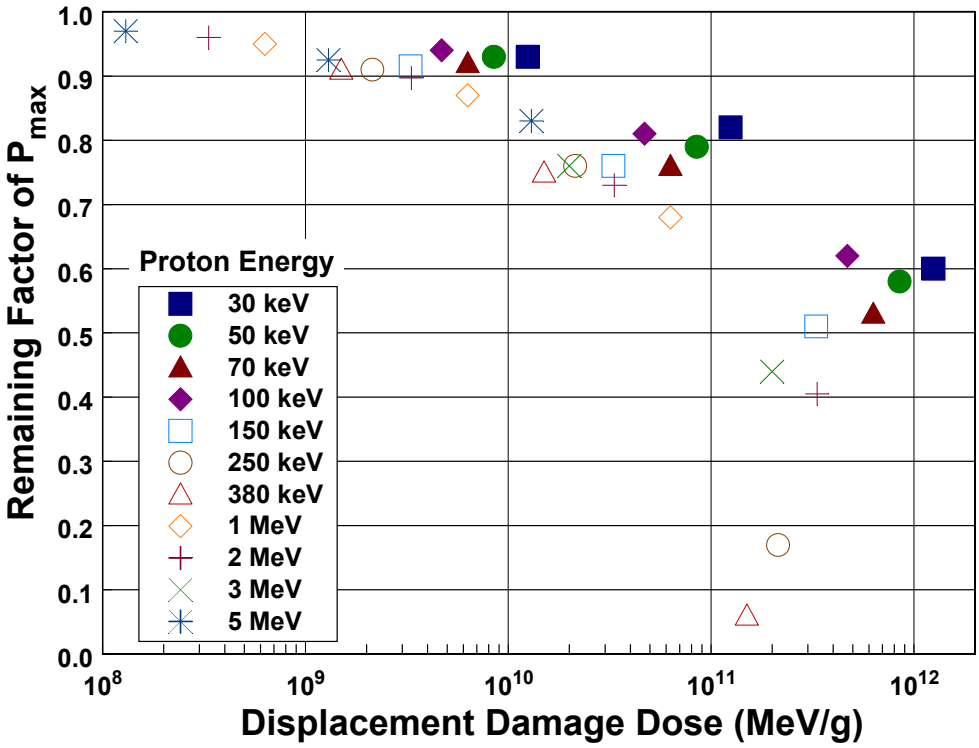

Figure 5: Data from Sumita et al. [17] showing 3J $InGaP_2$/GaAs/Ge degradation under proton irradiation.

The cells studied in [17] were optimized for radiation resistance, so the cells remained top cell limited for nearly all of the irradiations considered. Therefore, most of the variation in radiation response was confined to degradation in the open circuit voltage (V_{oc}). Notable examples are at the highest D_d values for the 0.25 and 0.38 MeV datasets. In these two cases, severe degradation is observed in the 3J cell output. This is the case because the Bragg peak for these protons lies within the GaAs subcell (Figure 4), and the GaAs subcell damage is so severe at these high D_d values that it becomes the current limiter and pulls down the overall 3J device output.

The response of the 3J solar cell to the non-uniform defect distribution induced by these unidirectional, monoenergetic irradiations can give the impression the that low energy protons are likely to cause the majority of the overall damage on-orbit. In fact, this is not the case for the reasons that we will discuss below.

4.2 Monoenergetic, Omnidirectional Protons

The second case modelled assumed the same incident proton energies as shown in Figure 4, except that the protons were assumed to be omnidirectional. This was accomplished using the user-defined input spectrum option of SRIM (TRIM.DAT) with all of the protons confined to a single energy. A separate algorithm was developed to produce the randomization of the incidence angle of each proton from 0 to 180° and tabulate it in terms of direction cosines in the x, y, and z directions conducive to the SRIM input file requirements. The vacancy production rates are shown in Figure 6.

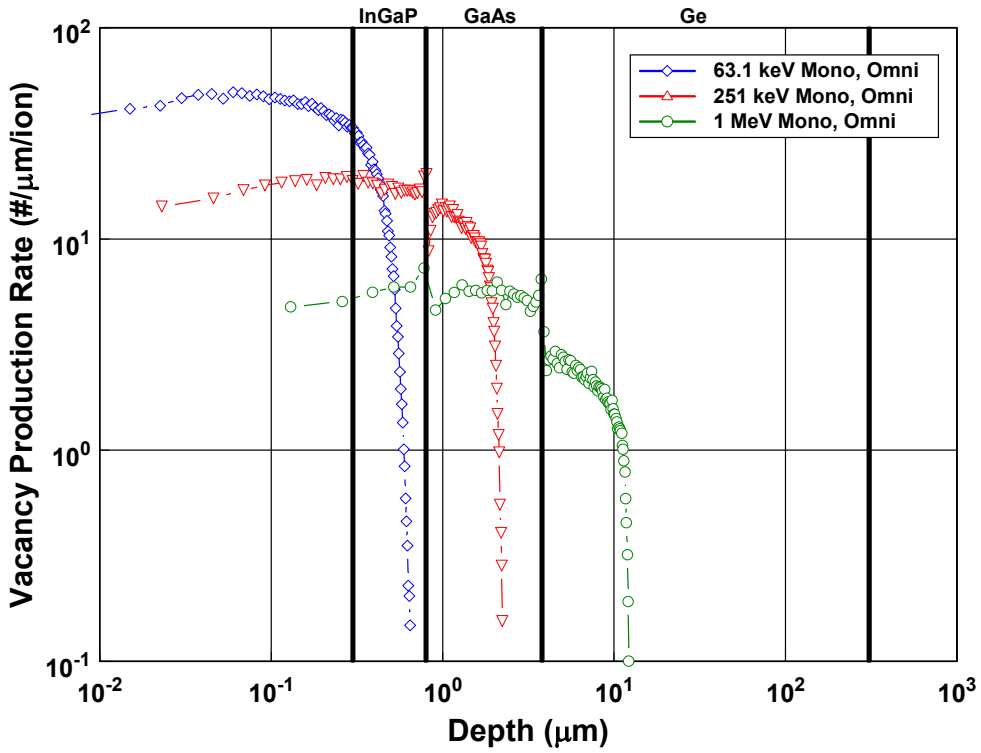

Figure 6: Vacancy production rates for omnidirectional, monoenergetic proton irradiations as calculated by SRIM using the input file TRIM.DAT.

In comparison with the unidirectional case of Figure 4, for each of the incident energies, the damage profile produced by an omnidirectional exposure is more uniform. In particular, while the end of the proton track occurs in the same region for each specific incident energy, no clear Bragg Peak is evident in the omnidirectional case. The localized damage peak induced by a unidirectional proton irradiation is removed when the irradiation is omnidirectional.

4.3 Omnidirectional Proton Spectrum

To complete the modelling, the case of an omnidirectional proton spectrum irradiation is considered. The calculations were set up just as was done for Figure 6 except that instead monoenergetic protons, we chose a proton spectrum from Figure 3. And, in order to simulate a typical application, we chose a 76.2 μm (3 mil) SiO_2 coverglass. Again, we are only considering front-side exposure in these calculations. The results are shown in Figure 7.

The results of Figure 7 show that exposure to the omnidirectional, isotropic, slowed-down spectrum causes a much more uniform damage distribution throughout the solar cell active region. Also, the absolute amount of damage produced is significantly less than the first two cases modelled, which is a result of the shielding provided by the coverglass.

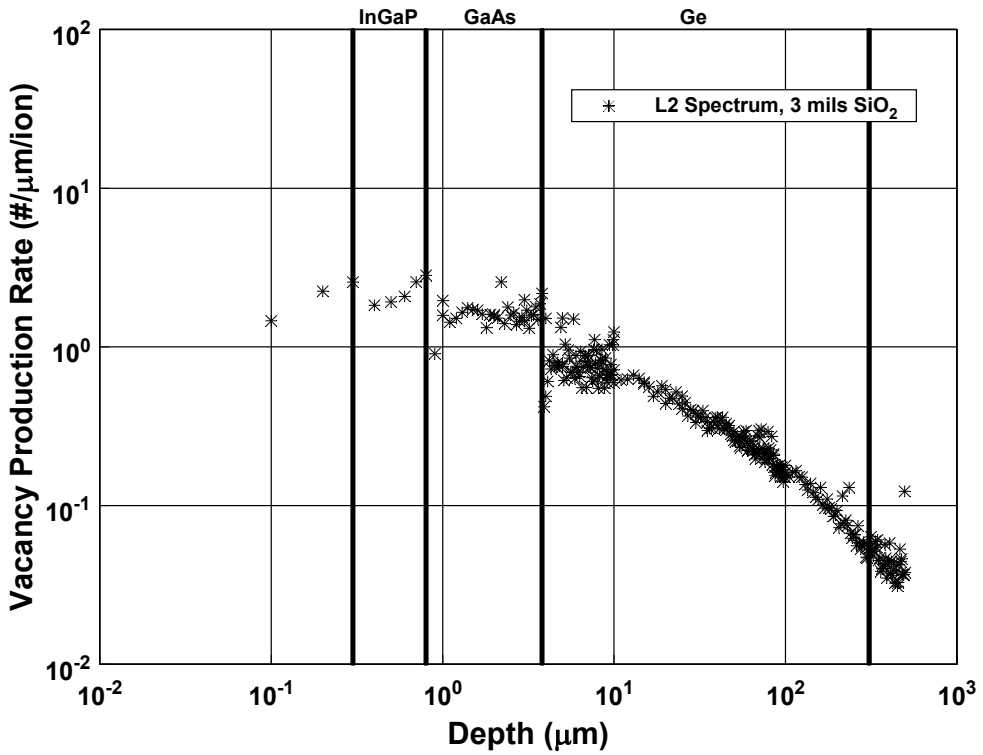

Figure 7: Vacancy production rate induced by an omnidirectional spectrum of protons that have been slowed-down by a 76.2 μm (3 mil) coverglass.

5. DISCUSSION

The ultimate goal of the present analysis is to gain insight into the proper method for predicting the performance of the 3J $InGaP_2$/GaAs/Ge solar cell in a proton-dominated space radiation environment. The basic theory of displacement damage (Section 2) indicates that the damage increases with decreasing proton energy, and with a typical space proton spectrum being weighted towards lower energies (Figure 3), it may seem reasonable to base on-orbit predictions on ground tests made at relatively low proton energies. However, this is inappropriate for two reasons. Firstly, Figure 3 shows that the effect of a coverglass is to attenuate the overall proton fluence and to shift the distribution of proton energies arriving at the surface of the cell to higher energies. Secondly, the finite proton range, the different radiation sensitivity of each subjunction, and the geometry of the 3J device complicates the analysis of low energy proton data, as evidenced by the data from [16,17].

Fortunately, the analysis presented here shows that the effects brought on by the highly non-uniform damage distribution induced by unidirectional, monoenergetic proton irradiations are not likely to be observed on-orbit. Instead, exposure to the isotropic, omnidirectional spectrum of space after attenuation by the coverglass (Figure 7) will induce nearly homogeneous degradation throughout the cell active region.

There is some decrease in the damage profile with depth into the cell, but considering that the active region of the Ge does not extend much beyond 10 μm, the variation is no more than a factor of 2. Furthermore, the effect of backside irradiation has not been considered. Such irradiation will induce a damage profile of the same structure but decreasing toward the front of the cell. Since the rear shielding is typically much thicker, the addition to the total damage will be relatively small, but the backside irradiation will serve to further homogenize the damage profile. In the end, the damage profile throughout the cell active region is expected to vary by less than a factor of 2, and the variation will be gradual throughout the cell active region.

It follows, then, that on-orbit solar cell performance predictions can be based on a ground radiation test that produces a homogeneous defect profile. For the proton dominated orbit considered here, this can be readily achieved using standard monoenergetic, unidirectional proton irradiations provided that the incident proton energy is large enough that the proton loses minimal energy as it passes through the active region. From Figure 4 it is seen that any energy of a few MeV would be appropriate. Note that the combined effects of protons and electrons can also be calculated as a function of D_d [2].

Any higher proton energy could be used except for two caveats. First, the slope of the NIEL curve decreases above 10 MeV due to the onset of nuclear effects. Second, a discrepancy between the damage coefficients and the NIEL has been observed for incident proton energies above 10 MeV [19]. Also, it has been shown that ~ 80% of the degradation of a shielded GaAs solar cell in a space proton environment is induced by protons with incident energies between 1 and 10 MeV [12,13]. Thus, an energy between 1 and 10 MeV may be most appropriate for ground testing.

The usefulness of the present analysis is clearly seen when the radiation response is analyzed in terms of D_d. Within the D_d methodology, the space radiation environment is expressed as an equivalent value of D_d that is determined by an integral over energy of the product of the slowed-down spectrum (Figure 3) with the NIEL. The cell degradation in that environment can then be predicted from the characteristic degradation curve for the specific cell technology expressed in terms of D_d. This characteristic curve can be determined from a single ground test at any proton energy provided the energy is chosen appropriately as discussed above. Thus, qualification of a cell technology for a space proton radiation environment can, in principle, be reduced to a ground test at a single proton energy.

It is instructive to study how these effects are included in the equivalent fluence methodology developed by NASA's Jet Propulsion Laboratory (JPL) [5,5], which serves as the industry standard analysis technique. This method uses a set of empirically determined relative damage coefficients (RDCs) to correlate the radiation damage produced by different particles at different energies. An RDC relates the fluence of a given particle at a given energy required to produce a certain degradation level to the fluence of a different particle and energy required to produce an equal amount of degradation. The RDCs are determined from monoenergetic, unidirectional irradiations on unshielded solar cells, and the omnidirectional nature of the space spectrum and shielding effects are compensated for by analytically modifying the RDCs.

The modification of the RDCs consists of an integral over the solid angle above the solar cell. For those protons with incident energy large enough to pass through the coverglass and cell active region with minimal energy loss, the integral reduces by a factor of 2. For protons of lower incident energy, the integral is modified to account for the finite range of the proton. This is the reason for the two terms in the integral of Eq. 5-13 of [5]. The result is a reduction of the unidirectional RDCs.

These effects can be seen in a comparison of the unidirectional and omnidirectional RDCs for the case of an unshielded solar cell. For a fully penetrating proton, e.g. 10 MeV, the omnidirectional RDC is one-half the unidirectional value. For a 0.1 MeV proton, however, the unidirectional RDC is reduced by a factor of more than 5 [5]. Thus, even without a coverglass, the omnidirectional nature of the space environment results in a significant reduction in the impact of the low energy content of the proton spectrum. The addition of shielding effectively truncates the incident spectrum over which damage is produced. This fact tells us that the use of low energy, normally incident, proton irradiations are not needed to calculate the omnidirectional RDCs for most practical applications using the JPL equivalent fluence method. For example, one only need define the normally-incident, uncovered RDCs to energies >1 MeV to generate omnidirectional RDCs for a 1 mil coverglass case.

6. CONCLUSIONS

From this analysis, it is concluded that, in a typical operational space environment, an MJ solar cell will experience an approximately uniform damage distribution throughout the active region. The implications of this conclusion are two-fold. First, low energy proton irradiation ground testing is not likely to significantly improve the accuracy of the results if the cell degradation is analyzed in terms of displacement damage dose. Second, any preferential degradation of one subcell over another will be due primarily to the relative radiation sensitivities of the different subcell materials rather than non-uniform damage distribution.

7. ACKNOWLEDGEMENTS

The authors gratefully acknowledge Dr. Hugh Evans of ESTEC in the SPENVIS and MULASSIS calculations. We also acknowledge our extremely productive, ongoing collaboration with Drs. Mitsuru Imaizumi and Taishi Sumita of JAXA.

8. REFERENCES

[1] J. F. Ziegler, J. B. Biersack, and U. Littmark, The Stopping and Range of Ions in Solids, Pergammon, New York, 1985, Vol. 1.
[2] S .R. Messenger, G. P. Summers, E. A. Burke, R. J. Walters, and M. A. Xapsos, Prog. Photovolt: Res. Appl., **9**, 103 (2001)
[3] G. P. Summers, R. J. Walters, M. A. Xapsos, E. A. Burke, S. R. Messenger, P. Shapiro, and R. L. Statler, Proc. IEEE World Conf. Photo. Energy Conv., Hawaii, Dec 5-9, 1994, p. 2068.
[4] H.Y. Tada, J.R. Carter, Jr., B.E. Anspaugh, and R.G. Downing, JPL Publication 82-69, 1982.
[5] B. E. Anspaugh, JPL Publication 96-9, 1996.
[6] B. D. Weaver and R. J. Walters, Recent Res. Devel. Applied Phys., **6**, 747 (2003)
[7] E. A. Burke, IEEE Trans. Nuc. Sci. **33**, 1276 (1986)
[8] I. Jun, M.A. Xapsos, S.R. Messenger, E.A. Burke, R.J. Walters, G.P. Summers and T. Jordan, IEEE Trans. Nucl. Sci. **50**, 1924, 2003.
[9] http://reat.space.qinetiq.com/mulassis/
[10] http://www.spenvis.oma.be/spenvis
[11] H.Y. Tada, J.R. Carter, Jr., B.E. Anspaugh, and R.G. Downing, JPL Publication 82-69, 1982.
[12] G.P. Summers, S.R. Messenger, E.A. Burke, M.A. Xapsos, and R.J. Walters, Appl. Phys. Lett. **71**, 832 (1997)
[13] S.R. Messenger, M.A. Xapsos, E.A. Burke, R.J. Walters, and G.P. Summers, IEEE Trans. Nucl. Sci. **44**, 2169 (1997).
[14] F. Lei, P.R. Truscott, C.S. Dyer, B. Quaghebeur, D. Heynderickx, P. Nieminen, H. Evans, and E. Daly, IEEE Trans. Nucl. Sci. **49**, 2788 (2002).
[15] S. R. Messenger, E. A. Burke, G. P. Summers, and R. J. Walters, IEEE Trans. Nuc. Sci., 49, 2690 (2002)
[16] S. R. Messenger, E. A. Burke, R. J. Walters, J. H. Warner, and G. P. Summers, Prog. Photovolt: Res. Appl., **13**, 115 (2005)
[17] T. Sumita, M. Imaizumi, S. Matsuda, T. Ohshima, A. Ohi, and T. Kamiya, Proc. 19th Euro. Photo. Sci. and Eng. Conf., Paris, France, June, 2004.
[18] R. J. Walters, S. R. Messenger, and G. P. Summers, Proc. 28th IEEE Photo. Spec. Conf., Anchorage, AK, Sept, 2000, p. 1097
[19] J. H. Warner, R. J. Walters, S. R. Messenger, G. P. Summers, S. M. Khanna, D. Estan, L. S. Erhardt, and A. Houdayer, IEEE Trans. Nuc. Sci. **51**, 2887 (2004)